



Research Article

Allitol bioproduction by recombinant *Escherichia coli* with NADH regeneration system co-expressing ribitol dehydrogenase (RDH) and formate dehydrogenase (FDH) in individual or in fusion



Xin Wen ^a, Huibin Lin ^b, Yilin Ren ^c, Can Li ^d, Chengjia Zhang ^a, Jianqun Lin ^{a,*}, Jianqiang Lin ^{a,*}

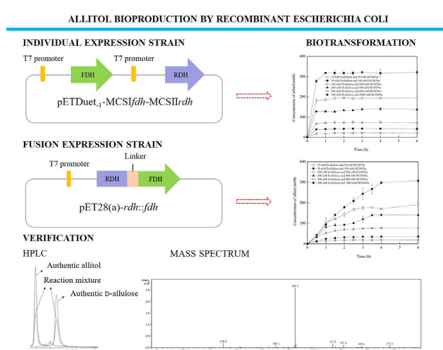
^a State Key Laboratory of Microbial Technology, Shandong University, Qingdao, China

^b Shandong Academy of Chinese Medicine, Jinan, China

^c Qingdao Longding Biotech Limited Company, Qingdao, China

^d School of Biological Engineering, Qilu University of Technology, Jinan, China

GRAPHICAL ABSTRACT



ARTICLE INFO

Article history:

Received 8 July 2021

Accepted 29 November 2021

Available online 3 December 2021

Keywords:

Allitol
Bioproduction
Co-expression
Cofactor recycle
D-Allulose
Formate dehydrogenase
Fusion expression
NADH regeneration system
Recombinant *Escherichia coli*
Ribitol dehydrogenase
Sugar alcohol

ABSTRACT

Background: As a kind of rare sugar alcohol, allitol has important application values in food and medication. In addition, it can be used as a key substrate to produce other D/L-rare sugars. Allitol can be effectively produced by the resting-cell biotransformation method.

Results: Two recombinant *Escherichia coli* strains, one simultaneously expressing ribitol dehydrogenase (RDH) and formate dehydrogenase (FDH) in fusion (fusion expression strain for short) and the other expressing the above two enzymes individually (individual expression strain for short), were respectively constructed and used for allitol bioproduction. The produced allitol was confirmed by HPLC, mass spectrometry, and polarimetry. The individual expression strain had higher activity, which produced 58.5 g/L allitol from 90 g/L D-allulose (also named D-psicose) in 1 h with an allitol productivity of 58.5 g/L/h under optimized conditions.

Conclusions: The constructed individual expression strain had the highest allitol productivity among the reports. The production process developed in this study was simple, highly efficient, and had the potential for mass production of allitol.

How to cite: Wen X, Lin H, Ren Y, et al. Allitol bioproduction by recombinant *Escherichia coli* with NADH regeneration system co-expressing Ribitol Dehydrogenase (RDH) and Formate Dehydrogenase (FDH) in individual or in fusion. *Electron J Biotechnol* 2022;55. <https://doi.org/10.1016/j.ejbt.2021.11.007>

© 2021 Pontificia Universidad Católica de Valparaíso. Production and hosting by Elsevier B.V. This is an open access article under the CC BY-NC-ND license (<http://creativecommons.org/licenses/by-nc-nd/4.0/>).

* Corresponding authors.

E-mail addresses: jianqunlin@sdu.edu.cn (J. Lin), jianqianglin@sdu.edu.cn (J. Lin).

1. Introduction

Allitol is a six-carbon rare sugar alcohol that can be used as a sweetener and a bulking agent in the food industry [1]. Allitol also has important physiological functions. It can increase the water content in the small intestine and promote small intestinal transport so as to have a laxative effect and is used in the preparation of monosaccharide laxatives for the treatment of constipation [2]. Allitol is an important intermediate in the synthesis of azasugars, which can be used in the preparation of drugs against diabetes, cancer, and viral infections including AIDS [1]. Furthermore, allitol can be used as a substrate to produce other D/L-type rare sugars, such as D/L-allulose (also named D/L-psicose), according to Izumoring strategy [3,4,5].

Allitol is rare in nature and difficult to obtain from natural resources. It can be chemically synthesized, but has a low yield and toxic byproducts [1,6]. In contrast, the biotransformation method is more suitable as it has many advantages, such as mild reaction conditions, no side products, low pollution to the environment, low cost, and high yield, etc. Allitol can be biotransformed from D-allulose by ribitol dehydrogenase (RDH) consuming NADH. The expensive coenzyme, NADH, plays an important role in oxidoreductase reactions, and can be regenerated by using enzyme or microbial technology [7,8,9,10]. In this research, formate dehydrogenase (FDH) is used for NADH regeneration, utilizing formate in the production of allitol (Fig. 1). As a coenzyme regeneration system, formate dehydrogenase has the following advantages: first, the reduction reaction catalyzed by formate dehydrogenase is irreversible; second, the required substrate formate is cheap and has little negative effect on the enzyme activity; and third, the by-product of carbon dioxide (CO₂) produced has little negative effect on the enzyme activity, and is easily spilled from the reaction system, which simplifies the product separation and purification [11].

Allitol bioproduction from D-allulose by using enzymatic catalysis and resting-cell biotransformation methods has been reported [12,13,14,15]. But the production was too low for real applications. In natural cells, enzymes are arranged in order rather than distributed randomly in the cell space. This ordered arrangement makes the enzyme molecules of the same metabolic pathway close to each other to overcome the diffusion limit of intermediate metabolites and the crosstalk of intermediate products of different metabolic pathways. Co-expressing RDH and FDH in an individual is a normal way, but in which expression mode the expressed RDH and FDH enzyme molecules could be far from each other inside the host cell and the intermediate metabolite of one enzyme needs to diffuse to the other enzyme to finish one reaction cycle, as shown

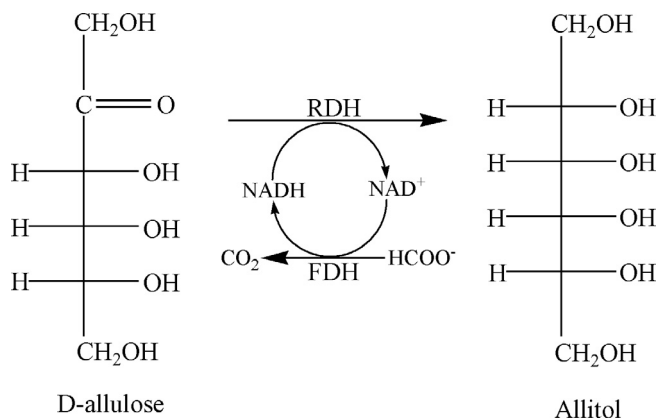


Fig. 1. Conversion diagram of allitol from D-allulose by using RDH and FDH with NADH regeneration. RDH, ribitol dehydrogenase; FDH, formate dehydrogenase.

in Fig. 1. The diffusion of the intermediate metabolite may also interfere with the metabolism of the host cells. Fusion expression is a simple method of enabling two recombinant proteins close to each other. Thus, fusion expression of RDH and FDH was investigated in this research and compared with the individual expression strain.

Even if the substrate of D-allulose is a rare sugar, it can be produced from the cheap substrate D-fructose or D-glucose by some labs, including ours [16,17,18,19,20,21,22,23,24]. Therefore, D-allulose was used in the bioproduction of allitol in this research. According to the reports, the RDH from *Providencia alcalifaciens* RIMD 1656011 had high specificity and almost no by-products in catalyzing D-allulose into allitol [1,13], and was therefore used in this research. The consumed NADH in allitol production can be regenerated by FDH [25,26]. The FDH from *Pseudomonas* sp. 101 was reported to be stable [27] and was used in this research. Two gene expression strategies were used in constructing the recombinant strains co-expressing RDH and FDH in individual or fusion and the conditions for biocatalyst preparation and allitol biotransformation were optimized. Finally, 58.5 g/L of allitol was produced from 90 g/L of D-allulose, consuming 68 g/L of sodium formate for NADH regeneration by using the individual expression strains as biocatalysts. Allitol production was the highest among the reports, and the production process was simple and practical for large-scale production of allitol.

2. Materials and methods

2.1. Reagents, strains, plasmids, and primers

Allitol was purchased from TCI Development (Shanghai, China). Sodium formate was purchased from Macklin (Shanghai, China). D-Allulose was produced by our lab [17]. The bacterial strains, plasmids, and primers used in this study are listed in Table 1.

2.2. Construction of recombinant *E. coli* strains expressing RDH or RDH and FDH

The only RDH-expressing recombinant strain named *E. coli* BL21 (DE3)-pETDuet₁-MCSII_{rdh} was obtained by inserting the pETDuet₁-MCSII_{rdh} into the competent cell *E. coli* BL21 (DE3). The recombinant strain named *E. coli* BL21 (DE3)-pET28(a)-*rdh*, which only expresses RDH, was constructed as follows: the *rdh* fragment was cloned by using pETDuet₁-MCSII_{rdh} as the template and *rdh*-pET28(a)-NcoI-U and *rdh*-pET28(a)-XhoI-D as the primers; and the cloned *rdh* gene fragment was then inserted into pET28(a) using NcoI and XhoI restriction sites; and finally, the obtained plasmid named pET28(a)-*rdh* was transformed into *E. coli* BL21 (DE3) to construct *E. coli* BL21 (DE3)-pET28(a)-*rdh*. The primers used in this study are listed in Table 1.

In constructing the recombinant strain that expresses the fused RDH and FDH named *E. coli* BL21 (DE3)-pET28(a)-*rdh::fdh* (fusion expression strain for short), the *rdh* fragment without TAA at C-terminus was cloned by using pETDuet₁-MCSII_{rdh} as the template and *rrdh*-pET28(a)-NcoI-U and *rrdh*-pET28(a)-D as the primers. Likewise, the *fdh* fragment was cloned by using pETDuet₁-MCSII_{fdh} as the template and *rfdh*-pET28(a)-U (containing linker: GGATCTGGC) and *rfdh*-pET28(a)-XhoI-D as the primers. Then, the cloned *rdh* and *fdh* fragments were used as the common templates to clone the fusion gene fragment *rdh::fdh* by using *rrdh*-pET28(a)-NcoI-U and *rfdh*-pET28(a)-XhoI-D as the primers. Finally, the *rdh::fdh* fusion gene fragment was inserted into pET28(a) by using NcoI and XhoI restriction sites. The obtained plasmid was named pET28(a)-*rdh::fdh* and was transformed into *E. coli* BL21 (DE3) to construct *E. coli* BL21 (DE3)-pET28(a)-*rdh::fdh*.

Table 1
Strains, plasmids, and primers used in this study.

Plasmids, strains and primers	Characteristics, sources and sequences
Plasmids	Relevant characteristics
pET28(a)	Km ^r , T7 promoter
pETDuet ₁	Amp ^r , two multiple cloning sites
pETDuet ₁ -MCSII rdh	<i>rdh</i> , Amp ^r
pETDuet ₁ -MCSII fdh	<i>fdh</i> , Amp ^r
pET28(a)- <i>rdh</i>	<i>rdh</i> , Km ^r
pET28(a)- <i>rdh::fdh</i>	<i>rdh::fdh</i> , Km ^r
pETDuet ₁ -MCSII fdh -MCSII rdh	<i>fdh</i> , <i>rdh</i> , Amp ^r
Strains	Relevant characteristics
<i>E. coli</i> DH5 α	For gene cloning
<i>E. coli</i> BL21 (DE3)	For gene expression
<i>E. coli</i> BL21 (DE3)-pET28(a)	Containing pET28(a)
<i>E. coli</i> BL21 (DE3)-pETDuet ₁	Containing pETDuet ₁
<i>E. coli</i> BL21 (DE3)-pETDuet ₁ -MCSII rdh	RDH
<i>E. coli</i> BL21 (DE3)-pET28(a)- <i>rdh</i>	RDH
<i>E. coli</i> BL21 (DE3)-pET28(a)- <i>rdh::fdh</i>	Fusion expression strain; RDH::FDH
<i>E. coli</i> BL21 (DE3)-pETDuet ₁ -MCSII fdh -MCSII rdh	Individual expression strain; RDH; FDH
Primers	Sequences (5'-3')
<i>rdh</i> -pET28(a)- <i>Nco</i> I-U	CATGCCATGGCCATTAGCCTGGAAAATAAGGTGG
<i>rdh</i> -pET28(a)- <i>Xho</i> I-D	CCGCTCGAGTTAATGGTGATGATGATGATGCAGATCAACA
	CTATTCGGCAG
<i>rrdh</i> -pET28(a)- <i>Nco</i> I-U	CATGCCATGGCCATTAGCCTGGAAAATAAGGTGG
<i>rrdh</i> -pET28(a)-D	CAGATCAACACTATTCGGCAGAATAAC
<i>rfdh</i> -pET28(a)-U	GTTATTCTGCCAATAGTGTGATCTGGGATCTGGCATGG
	CAAAGTGCTGTGCGTGTGTATG
	CCGCTCGAGTTAATGGTGATGATGATGATGCACGGCTTTT
	TGAATTTTGTGCTTC
<i>fdh</i> -pETDuet ₁ -MCSII- <i>Nco</i> I-U	CATGCCATGGCAAAGTGCTGTGCGTGTGT
<i>fdh</i> -pETDuet ₁ -MCSII- <i>Not</i> I-D	AAGGAAAAAGCGGCCACGGCTTTTGAATTTTGTCT
	GCTTCTTCG

Primers: restriction sites were indicated with italic and linker was indicated with underline.

In constructing the recombinant strain expressing RDH and FDH in an individual named *E. coli* BL21 (DE3)-pETDuet₁-MCSII fdh -MCSII rdh (individual expression strain for short), the *fdh* fragment was cloned by using pETDuet₁-MCSII fdh as the template, and *fdh*-pETDuet₁-MCSII-*Nco* I-U and *fdh*-pETDuet₁-MCSII-*Not* I-D as the primers. Then the *fdh* gene fragment was inserted into pETDuet₁-MCSII rdh by using *Nco*I and *Not*I restriction sites to form the plasmid pETDuet₁-MCSII fdh -MCSII rdh . Finally, the plasmid was transformed into *E. coli* BL21 (DE3) to construct *E. coli* BL21 (DE3)-pETDuet₁-MCSII fdh -MCSII rdh .

2.3. Cultivation media and conditions

Seed culture was performed using 50 mL flasks containing 10 mL LB medium (1% tryptone, 0.5% yeast extract, and 1% NaCl) cultured at 37°C and 200 rpm for 12 h. Cell biocatalysts cultivation was performed using 500 mL flasks containing 100 mL of LBG medium (LB medium supplied with 5 g/L glucose) with 1 mL inoculation, started at 37°C and 200 rpm. After 3 h of cultivation, IPTG was added to the final concentration of 1 mM and the conditions changed to 28°C, 140 rpm, and continued the cultivation for a further 12 h. Kanamycin or ampicillin was added to the final concentration of 100 µg/mL in the initial medium.

2.4. Resting-cell biotransformation

The recombinant *E. coli* cells were harvested by centrifugation at 12,000 × g for 5 min and washed twice by using double distilled water. The washed cells were resuspended in a reaction solution containing 50 mM Tris-HCl buffer, 50 mM D-allulose, and 100 mM sodium formate. The reaction was operated at 35°C (before temperature optimization) or the optimized value and pH 7.0 (before pH optimization), or the optimized value. All trials were performed in triplicates.

2.5. Analytical methods

Allitol was identified by using high performance liquid chromatography (HPLC), mass chromatography, and optical rotation. The qualitative and quantitative analyses of allitol and D-allulose were measured by using HPLC at a column temperature of 78°C and eluted with double distilled water at a flow rate of 0.5 mL/min using a Carbomix Pb-NP column (7.8 × 300 mm, 10 µm, Sepax Technologies). A mass spectrometry (BRUKER, Germany) was performed in negative ion detection mode with an ESI ion source. Around 5 µL allitol of 10 µg/mL (dissolved in double distilled water) was injected and eluted at a flow rate of 0.4 mL/min. The optical rotation of allitol (5% in double distilled water) was determined by using a polarimeter (INESA, China) at 25°C.

3. Results

3.1. Expression of proteins RDH, FDH, and RDH::FDH

For analyses of the expression of the recombinant proteins, the above two recombinant *E. coli* strains, *E. coli* BL21 (DE3)-pET28(a)-*rdh::fdh* or *E. coli* BL21 (DE3)-pETDuet₁-MCSII fdh -MCSII rdh , and the two control *E. coli* strains containing empty plasmid pET28(a) or pETDuet₁ were, respectively, cultivated in LB medium induced by IPTG for 5 h. The cells were harvested by centrifugation at 12,000 × g for 5 min, and the intracellular proteins were extracted for analyses. SDS-PAGE analyses of the total proteins from the *rdh::fdh* fusion expression strain showed a protein band around 71 kDa (Fig. 2A), and that of the *fdh* and *rdh* individual expression strain showed two protein bands around 45 kDa and 26 kDa, respectively (Fig. 2B). The RDH molecular weight was consistent with the report [13].

In order to verify that the expressed FDH had real function in the biotransformation, we compared the allitol yield produced at

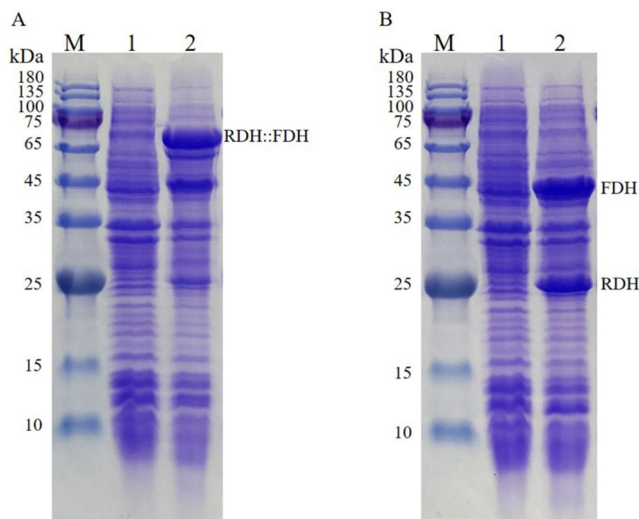


Fig. 2. SDS-PAGE analyses of fusion protein RDH::FDH (A) and individual expression proteins of FDH and RDH (B), respectively, expressed by *E. coli* BL21 (DE3). A: Lane M, protein marker; lane 1, the total proteins of *E. coli* BL21 (DE3)-pET28(a); lane 2, the total proteins of *E. coli* BL21 (DE3)-pET28(a)-*rdh::fdh*; B: Lane M, protein marker; lane 1, the total proteins of *E. coli* BL21 (DE3)-pETDuet.1; lane 2, the total proteins of *E. coli* BL21 (DE3)-pETDuet.1-MCS1*fdh*-MCS1*rdh*.

OD₆₀₀ 40 by the co-expression strains to the control strains expressing only RDH. The results showed that allitol production increased by about 8.5 or 8.3 times by using the individual expression strain or fusion expression strain, respectively, compared with the corresponding controls (Fig. 3).

3.2. Identification of allitol

The allitol produced was purified by cooling crystallization and recrystallization before identification. The result of HPLC analysis shown in Fig. 4A showed that the retention time of allitol and D-allulose in the reaction mixture was the same as that of the authentic allitol and D-allulose. The result of the mass chromatography showed that the mass of the produced allitol was 182.1 from the mass spectrum (Fig. 4B, which was equal to the molecular weight of allitol and the report [14]). The result of the polarimetric analysis showed that the specific optical rotation of the produced

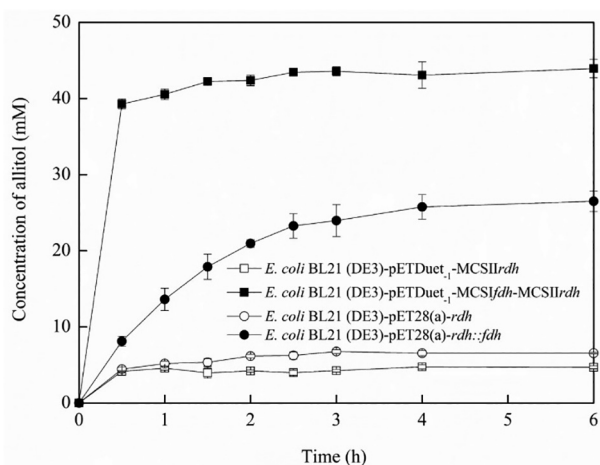


Fig. 3. The time courses of allitol production by using *E. coli* BL21(DE3)-pETDuet.1-MCS1*fdh*-MCS1*rdh* or *E. coli* BL21(DE3)-pET28(a)-*rdh::fdh* compared with the controls *E. coli* BL21(DE3)-pETDuet.1-MCS1*rdh* or *E. coli* BL21(DE3)-pET28(a)-*rdh*.

allitol was 0.0°, as expected. As a result, the produced product was confirmed to be allitol.

3.3. Optimization of medium carbon source for the cultivation of cell biocatalysts

The amounts of 1% (w/v) glucose, 1% (v/v) glycerol, and 1% glucose plus 1% glycerol were, respectively, added into the LB medium for cultivation of the catalytic cells, with the control without carbon source addition. After cultivation, cells were collected and allitol biotransformation was performed. The results indicated that the addition of carbon sources into the LB medium in the cultivation of the cells could increase allitol yield remarkably (Fig. 5A). The allitol yield reached its highest when 1% glucose or 1% glucose plus 1% glycerol were added into the cell cultivation medium. Taking into consideration the medium cost, only glucose was selected as the optimal carbon source. Then, glucose concentration was optimized using the individual expression strain, and the allitol yield was the highest when 5 g/L of glucose was added to the medium (Fig. 5B).

3.4. Optimization of pH, temperature, and cell mass for allitol biotransformation

The pH effect on allitol yield was investigated using four buffer systems of 50 mM, which were sodium acetate buffer (pH 4.0–6.0), sodium phosphate buffer (pH 6.0–8.0), tris-HCl buffer (pH 8.0–9.0), and glycine-NaOH buffer (pH 9.0–11.0), reacted at the optimal temperatures of 45°C for the fusion expression strain and 50°C for the individual expression strain, respectively. The results indicated that the highest allitol yield was obtained at pH 8.0 and pH 9.0 in 50 mM tris-HCl buffer for the fusion expression strain and individual expression strain, respectively (Fig. 6A).

The temperature effect on allitol production was investigated at various temperatures of 30, 35, 40, 45, 50, 55, and 60°C, respectively, using a reaction time of 0.5 h. The results showed that 45 and 50°C were optimal for the fusion expression strain and the individual expression strain, respectively (Fig. 6B).

The cell dosage effect on allitol yield was investigated at various cell concentrations with OD₆₀₀ 20, 40, 60, 80, and 100, corresponding to dry cell weights of 11.7, 23.3, 34.9, 46.5, and 58.0 g/L for the fusion expression strain and 14.7, 29.4, 44.0, 58.7, and 73.4 g/L for the individual expression strain, respectively. As shown in Fig. 6C, the optimal cell concentrations were OD₆₀₀ 40 and 80 for the individual expression strain and the fusion expression strain, respectively.

3.5. Optimization of D-allulose to sodium formate ratio for allitol biotransformation

The effect of D-allulose to sodium formate ratio (mM/mM) on allitol yield was investigated at ten values of 50:0, 50:1, 10:1, 5:1, 5:2, 5:4, 5:8, 1:2, 1:3, and 1:4, respectively, using the individual expression strain. The optimal D-allulose:sodium formate (mM/mM) ratio was 1:2 (Fig. 7A).

The effect of D-allulose concentration on allitol production of the two recombinant *E. coli* strains was investigated at six different D-allulose concentrations from 25 to 500 mM. For the fusion expression strain, the allitol concentration increased rapidly within the first 1 ~ 4 h for all D-allulose concentrations (Fig. 7B), while the allitol yields decreased from 88.1 to 61.5% as the D-allulose concentration increased from 25 mM to 500 mM. For the individual expression strain, the allitol concentration increased rapidly within the first 0.5 ~ 1 h, almost unchanged afterwards (Fig. 7C), and the

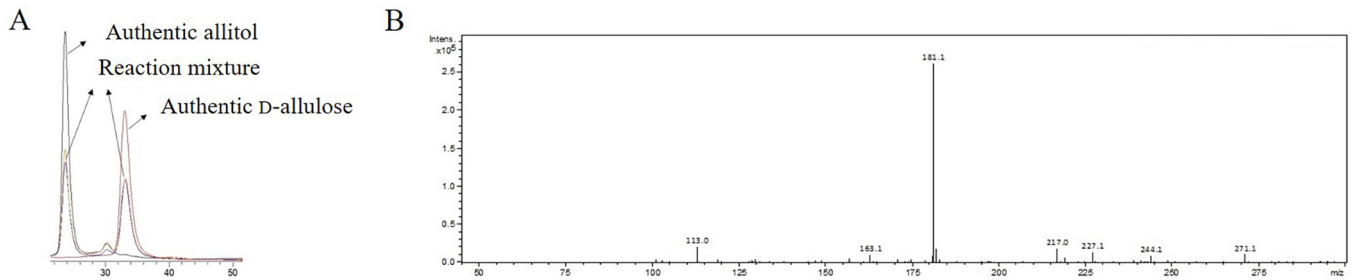


Fig. 4. HPLC analyses of authentic allitol, authentic D-allulose and the reaction mixture (A), and the mass spectrum of purified allitol product (B).

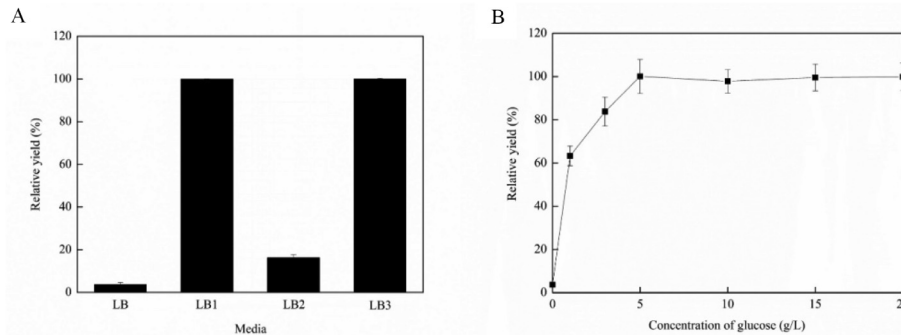


Fig. 5. The relative allitol yield obtained by the individual expression strain cultivated in LB medium supplied with various carbon sources (A) or at various glucose concentrations (B). LB1: LB medium containing 1% glucose; LB2: LB medium containing 1% glycerol; LB3: LB medium containing 1% glucose and 1% glycerol.

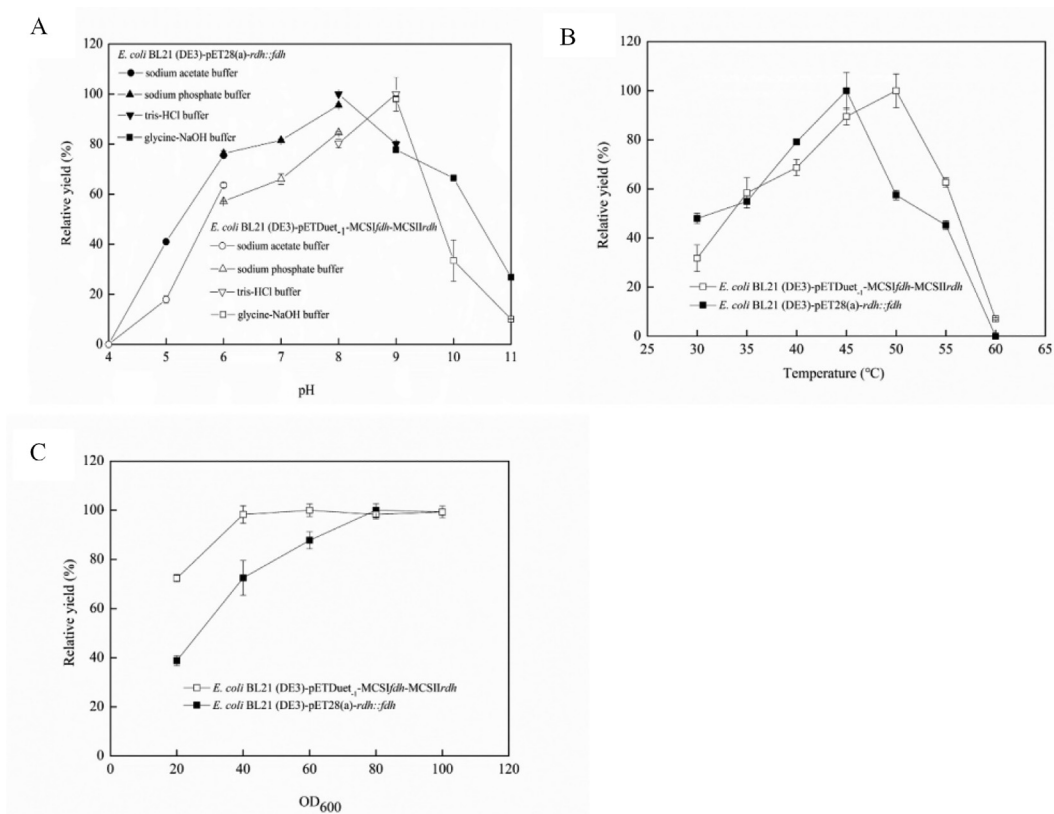


Fig. 6. Effects of pH (A), temperature (B) and cell concentration (C) on allitol relative yields for the fusion expression strain and individual expression strain.

allitol yields decreased from about 90.3 to 64.3% when the D-allulose concentration was increased from 25 mM to 500 mM. However, the cell concentration of the fusion expression strain

used in the biotransformation was about twice that of the individual expression strain to achieve a similar allitol yield. Overall, the individual expression strain had higher allitol biotransformation

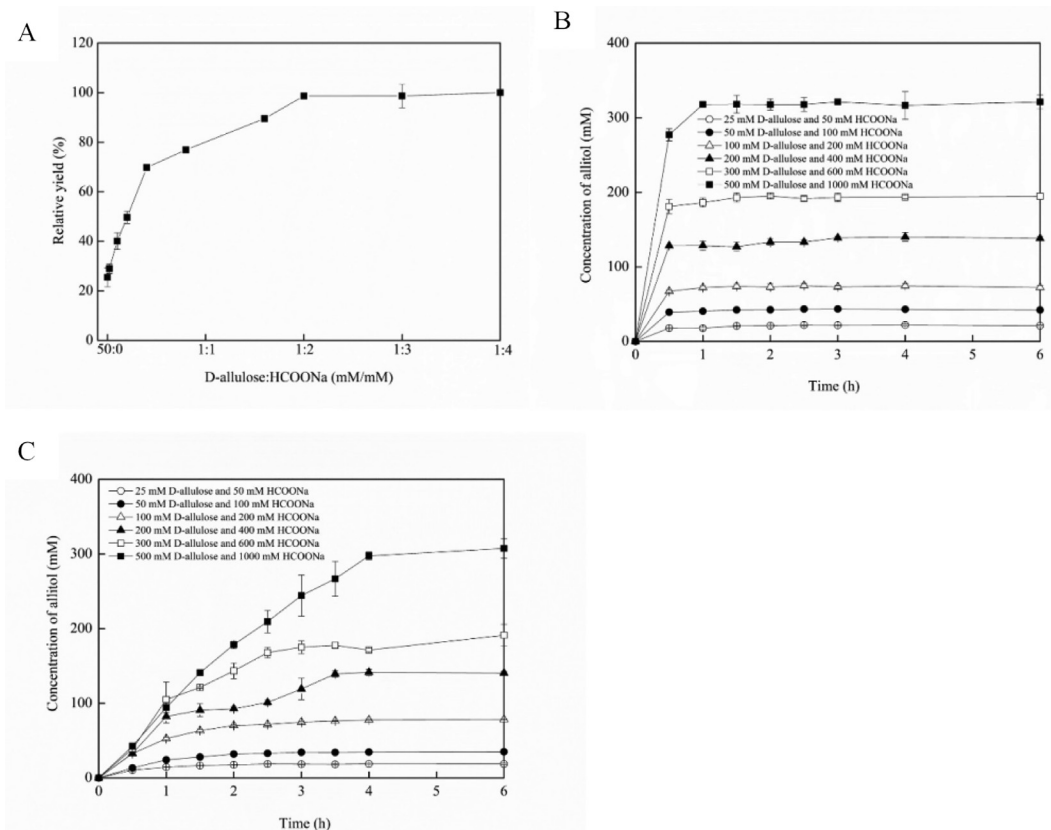


Fig. 7. Effects of D-allulose:HCOONa ratio (A) and the concentrations of D-allulose and HCOONa (B) on allitol relative yield of the individual expression strain at OD₆₀₀ 40, and effects of the concentrations of D-allulose and HCOONa on allitol relative yield of the fusion expression strain at OD₆₀₀ 80 (C).

activity. After 1 h of reaction, 58.5 g/L (321 mM) allitol and 6.5 g/L (36 mM) D-allulose remained in the reaction mixture with an allitol content of 90% (58.5/(58.5 + 6.5)) and a productivity of 58.5 g/L/h obtained at the conditions of OD₆₀₀ 40, initial D-allulose and sodium formate concentrations of 90 and 68 g/L, respectively. Crystallization can be applied after concentration of the reaction mixture to obtain allitol crystals.

4. Discussion

In this study, two recombinant strains used for allitol production from D-allulose were constructed. The produced allitol was purified and successfully confirmed by HPLC, mass spectrometry, and polarimetry.

The carbon source in the medium for cultivation of individual expression strains was optimized and glucose was found more effective than glycerol to improve the biotransformation rate. The reason may be that the addition of a suitable carbon source in the cultivation of the biocatalysts can increase the intracellular NADH concentration and further increase the biotransformation rate, which was supported by the reports [28,29].

The fusion expression method has the advantage of channeling the intermetabolites inside the cells, in which case, the product of the first enzyme is the substrate of the second enzyme, and vice versa, so as to increase the local substrate concentrations and avoid diffusion inside the cells to overcome the crossover effects of the intermetabolites in interference with the host cell metabolism [30]. However, the fusion expression strain of RDH::FDH had lower activity than the individual expression strain. The reason could be that the linker peptide (-Gly-Ser-Gly-) used is not suitable for the fusion of ribitol dehydrogenase and formate dehydrogenase. This

may lead to the independent deterioration of the two enzymes and may also lead to the misfolding and degradation of the fusion protein. In the future, other types of linker peptides, such as anti-protease degradation linker peptides that are rich in Pro-Thr, can be attempted [31,32,33,34]. In addition, the application of intracellular scaffold systems, including protein, DNA, and RNA scaffolds, which can realize co-regionalization of enzyme molecules, can also be tried to improve the fluidity of the protein, increase the local concentration of metabolites, and promote product synthesis [35,36,37,38].

It was reported that the optimum pH and the temperature stability of FDH from *Pseudomonas* sp.101 were 6.0–9.0 and 55°C, respectively [11,39]. The optimum pHs of the fusion expression strain (pH 8.0) and individual expression strain (pH 9.0) were all within the above pH range, while the optimum temperatures of the fusion expression strain (45°C) and individual expression strain (50°C) were lower than 55°C, which probably resulted from the RDH properties. Hassanin et al. reported that the optimum temperature and optimum pH of RDH from *Providencia alcalifaciens* RIMD 1656011 were 35°C and 10.0, respectively [13]. Taking into consideration the above facts, the optimum temperatures and pHs of the fusion expression strain (45°C, pH 8.0) and individual expression strain (50°C, pH 9.0) obtained in this study were reasonable. The disparity of the optimum temperature and optimum pH comes from the fusion expression strain and individual expression strain, which may be due to the different construction methods of the recombinant strains. In real applications, formic acid can be used in pH control in the production process to overcome the pH increase due to the consumption of formate and to provide the substrate for NADH regeneration as well [40]. Normally, sodium formate is chosen as the substrate for formate dehydrogenase (FDH) to realize the NADH regeneration. In order to boost the

Table 2
Allitol production from D-allulose by using enzymatic and whole cell biotransformation methods.

Biocatalyst	D-allulose (g/L)	NADH (NAD ⁺)	Temperature (°C)	pH	Time (h)	Productivity (g/L/h)	Reference
<i>Enzymes</i>							
RDH, FDH	10	+	30	8.0	48	0.2	[46]
RDH, FDH	10	+	40	7.5	6	1.4	[14]
<i>Strains</i>							
<i>Enterobacter agglomerans</i> Strain 221e	20	–	30	9.0	12	0.9	[29]
<i>Klebsiella oxytoca</i> G4A4	10	–	37	8.0	72	0.1	[12]
Engineered <i>E. coli</i>	20	–	30	7.0	12	0.7	[15]
Fusion expression strain	90	–	45	8.0	6	9.3	This study
Individual expression strain	90	–	50	9.0	1	58.5	This study

“+”, NADH(NAD⁺) was added into the reaction solution; “–”, no NADH(NAD⁺) was added into the reaction solution.

reaction with sufficient coenzyme NADH, the amount of sodium formate is usually excessive. Thus, the optimal D-allulose:sodium formate (mM/mM) ratio of 1:2 was achieved in this study.

Natural allitol mainly exists in *Itea* plants and *Tylophilus plumbeoviolaceus*. Only 14 g or 1.2 g of allitol can be extracted from 1 kg of fresh leaves of *Itea virginica* and 485 g fresh fruit of *T. plumbeoviolaceus*, respectively [41,42]. Allitol production by extraction from natural resources has the problems of consuming a large amount of raw materials, being harmful to the environment, and being expensive, which is not suitable for allitol's large-scale production. Allitol can also be chemically synthesized, and 11.3 g of allitol was obtained from the reaction mixture comprising 13 g of D-allose, 85 mL of water, and 4 g of sodium borohydride [1]. Although the chemical synthetic method has high efficiency, the substrate is also a rare sugar and is of high cost. Besides, the reaction process is complicated and produces by-products, making the product separation and purification difficult. Therefore, chemical synthesis is also not an ideal method. Table 2 shows the reported allitol productivities using the enzymatic catalysis and resting-cell biotransformation methods, respectively. As shown in Table 2, the allitol productivity of this study was up to 58.5 g/L/h without extra NADH/NAD⁺ addition, which was much higher than the reports. Overall, allitol production by using biotransformation methods developed in this study is environment-friendly, high-yielding, and economical, which can overcome the disadvantages of extraction and chemical synthetic methods, and is suitable for commercial production of allitol. In addition, the allitol portion in the reaction mixture was as high as 90%, which was high enough to be used for crystallization without further purification so as to simplify the product purification process and decrease the production cost [43]. In the future, further optimization of the biotransformation process will be carried out according to the reaction kinetics of the catalytic process of allitol production [44,45].

5. Conclusions

In this research, the recombinant strain co-expressing RDH and FDH in individual or in fusion showed higher allitol productivity compared with the reports. Between them, the individual expression strain had higher activity and was the highest among the reports, which produced 58.5 g/L allitol from 90 g/L D-allulose in 1 h with an allitol productivity of 58.5 g/L/h under optimized conditions. The reaction mixture contained 90% allitol, which could be used in crystallization without further purification so as to simplify the production process and decrease the production cost. The method developed in this research is practical for large-scale allitol production.

Financial support

This research was funded by the National Key Research and Development Program of China (2017YFC1701502, 2017YFC1701504, 2017YFC1702701), Taishan Scholar Project (ts201511107), Major increase and decrease projects of Central Government (2060302), Jinan Agricultural Application Technology Innovation Plan (CX202112), the Ecological Planting and Quality Assurance Project of Genuine Medicinal Materials, and China Postdoctoral Science Foundation (2021M701994).

Conflict of interest

No conflict of interest associated with this work.

Acknowledgments

We thank Mr. Chengjia Zhang and Ms. Caiyun Sun from the Core Facilities for Life and Environmental Sciences, State Key Laboratory of Microbial Technology, for help and guidance in the experiments.

References

- [1] Hassanin HAM, Mu W, Koko MYF, et al. Allitol: production, properties and applications. *Int J Food Sci Technol* 2016;52(1):91–7. <https://doi.org/10.1111/ijfs.13290>.
- [2] Oosaka K. Possible as monosaccharide laxative of rare sugar alcohols. *Yakugaku Zasshi* 2009;129(5):575–80. <https://doi.org/10.1248/yakushi.129.575>. PMID: 19420888.
- [3] Izumori K. Izumoring: a strategy for bioproduction of all hexoses. *J Biotechnol* 2006;124(4):717–22. <https://doi.org/10.1016/j.jbiotec.2006.04.016>. PMID: 16716430.
- [4] Takeshita K, Shimonishi T, Izumori K. Production of L-psicose from allitol by *Gluconobacter frateurii* IFO 3254. *J Ferment Bioeng* 1996;81(3):212–5. [https://doi.org/10.1016/0922-338X\(96\)82210-0](https://doi.org/10.1016/0922-338X(96)82210-0).
- [5] Poonperm W, Takata G, Ando Y, et al. Efficient conversion of allitol to D-psicose by *Bacillus pallidus* Y25. *J Biosci Bioeng* 2007;103(3):282–5. <https://doi.org/10.1263/jbb.103.282>. PMID: 17434433.
- [6] Jumde VR, Eisink NN, Witte MD, et al. C3 Epimerization of glucose, via regioselective oxidation and reduction. *J Org Chem* 2016;81(22):11439–43. <https://doi.org/10.1021/acs.joc.6b02074>. PMID: 27755870.
- [7] Binay B, Alagoz D, Yildirim D, et al. Highly stable and reusable immobilized formate dehydrogenases: promising biocatalysts for in situ regeneration of NADH. *Beilstein J Org Chem* 2016;12:271–7. <https://doi.org/10.3762/bjoc.12.29>. PMID: 26977186.
- [8] Alpdagtas S, Yücel S, Kapkaç HA, et al. Discovery of an acidic, thermostable and highly NADP⁺ dependent formate dehydrogenase from *Lactobacillus buchneri* NRRL B-30929. *Biotechnol Lett* 2018;40(7):1135–47. <https://doi.org/10.1007/s10529-018-2568-6>. PMID: 29777512.
- [9] Duman ZE, Duraksoy BB, Aktaş F, et al. High-level heterologous expression of active *Chaetomium thermophilum* FDH in *Pichia pastoris*. *Enzyme Microb Technol* 2020;137:. <https://doi.org/10.1016/j.enzmictec.2020.109552>. PMID: 32423672109552.
- [10] Alpdagtas S, Binay B. NADP⁺-dependent formate dehydrogenase: a review. *Biocatal Biotransfor* 2020;1–9. <https://doi.org/10.1080/10242422.2020.1865933>.

- [11] Zhang X, Zhu M, Han R, et al. A novel 3-phytosterone-9 α -hydroxylase oxygenation component and its application in bioconversion of 4-androstene-3,17-dione to 9 α -hydroxy-4-androstene-3,17-dione coupling with a NADH regeneration formate dehydrogenase. *Molecules* 2019;24(14):2534. <https://doi.org/10.3390/molecules24142534>. PMID: 31336696.
- [12] Han W, Zhu Y, Men Y, et al. Production of allitol from D-psicose by a novel isolated strain of *Klebsiella oxytoca* G4A4. *J Basic Microbiol* 2014;54(10):1073–9. <https://doi.org/10.1002/jobm.201300647>. PMID: 24771547.
- [13] Hassanin HAM, Wang X, Mu W, et al. Cloning and characterization of a new ribitol dehydrogenase from *Providencia alcalifaciens* RIMD 1656011. *J Sci Food Agric* 2016;96(8):2917–24. <https://doi.org/10.1002/jsfa.7589>. PMID: 26693956.
- [14] Hassanin HAM, Hamsidi R, Koko MYF, et al. Synthesis of allitol from D-psicose using ribitol dehydrogenase and formate dehydrogenase. *Trop J Pharm Res* 2016;15(12):2701–8. <https://doi.org/10.4314/tjpr.v15i12.23>.
- [15] Hassanin HAM, Eassa MA, Jiang B. Facile synthesis of bioactive allitol from D-psicose by coexpression of ribitol dehydrogenase and formate dehydrogenase in *Escherichia coli*. *J Food Bioact* 2018;4:117–122. [10.31665/JFB.2018.4.167](https://doi.org/10.31665/JFB.2018.4.167)
- [16] Mu W, Chu F, Xing Q, et al. Cloning, expression, and characterization of a D-psicose 3-epimerase from *Clostridium cellulolyticum* H10. *J Agr Food Chem* 2011;59(14):7785–92. <https://doi.org/10.1021/jf201356q>. PMID: 21663329.
- [17] Li C, Lin J, Guo Q, et al. D-psicose 3-epimerase secretory overexpression, immobilization, and D-psicose biotransformation, separation and crystallization. *J. Chem Technol Biot* 2018;93(2):350–7. <https://doi.org/10.1002/jctb.5360>.
- [18] Li C, Zhang C, Lin J, et al. Enzymatic fructose removal from D-psicose bioproduction model solution and the system modeling and simulation. *J Chem Technol Biot* 2018;93(5):1249–60. <https://doi.org/10.1002/jctb.5483>.
- [19] Men Y, Zhu Y, Zeng Y, et al. Co-expression of D-glucose isomerase and D-psicose 3-epimerase: development of an efficient one-step production of d-psicose. *Enzyme Microb Technol* 2014;64–65:1–5. <https://doi.org/10.1016/j.enzmictec.2014.06.001>. PMID: 25152409.
- [20] Li Z, Li Y, Duan S, et al. Bioconversion of D-glucose to D-psicose with immobilized D-xylose isomerase and D-psicose 3-epimerase on *Saccharomyces cerevisiae* spores. *J Ind Microbiol Biot* 2015;42(8):1117–28. <https://doi.org/10.1007/s10295-015-1631-8>. PMID: 26065389.
- [21] Chen X, Wang W, Xu J, et al. Production of D-psicose from D-glucose by co-expression of D-psicose 3-epimerase and xylose isomerase. *Enzyme Microb Technol* 2017;105:18–23. <https://doi.org/10.1016/j.enzmictec.2017.06.003>. PMID: 28756856.
- [22] Zhang W, Li H, Jiang B, et al. Production of D-allulose from D-glucose by *Escherichia coli* transformant cells co-expressing D-glucose isomerase and D-psicose 3-epimerase genes. *J Sci Food Agric* 2017;97(10):3420–6. <https://doi.org/10.1002/jsfa.8193>. PMID: 28009059.
- [23] Jiang S, Xiao W, Zhu X, et al. Review on D-allulose: in vivo metabolism, catalytic mechanism, engineering strain construction, bio-production technology. *Front Bioeng Biotechnol* 2020;8:26. <https://doi.org/10.3389/fbioe.2020.00026>. PMID: 32117915.
- [24] Wang J, Sun J, Qi H, et al. High production of D-psicose from D-fructose by immobilized whole recombinant *Bacillus subtilis* cells expressing D-psicose 3-epimerase from *Agrobacterium tumefaciens*. *Biotechnol Appl Biochem* 2021;1–12. <https://doi.org/10.1002/bab.2115>. PMID: 33533517.
- [25] Beerens K, Desmet T, Soetaert W. Enzymes for the biocatalytic production of rare sugars. *J Ind Microbiol Biotechnol* 2012;39(6):823–34. <https://doi.org/10.1007/s10295-012-1089-x>. PMID: 22350065.
- [26] Li Z, Gao Y, Nakanishi H, et al. Biosynthesis of rare hexoses using microorganisms and related enzymes. *Beilstein J Org Chem* 2013;9:2434–45. <https://doi.org/10.3762/bjoc.9.281>. PMID: 24367410.
- [27] Alekseeva AA, Fedorchuk VV, Zarubina SA, et al. The role of Ala198 in the stability and coenzyme specificity of bacterial formate dehydrogenases. *Acta Naturae* 2015;7(1(24)):60–9. <https://doi.org/10.32607/20758251-2015-7-1-60-69>. PMID: 25927002.
- [28] Muniruzzaman S, Kobayashi H, Izumori K. Production of D-talitol from D-tagatose by *Aureobasidium pullulans* strain 113B. *J Ferment Bioeng* 1994;78(5):346–50. [https://doi.org/10.1016/0922-338X\(94\)90278-X](https://doi.org/10.1016/0922-338X(94)90278-X).
- [29] Muniruzzaman S, Tokunaga H, Izumori K. Conversion of D-psicose to allitol by *Enterobacter agglomerans* strain 221e. *J Ferment Bioeng* 1995;79(4):323–7. [https://doi.org/10.1016/0922-338X\(95\)93989-W](https://doi.org/10.1016/0922-338X(95)93989-W).
- [30] Aalbers FS, Fraaije MW. Enzyme fusions in biocatalysis: coupling reactions by pairing enzymes. *ChemBioChem* 2019;20(1):20–8. <https://doi.org/10.1002/cbic.201800394>. PMID: 30178909.
- [31] Hölsch K, Weuster-Botz D. Enantioselective reduction of prochiral ketones by engineered bifunctional fusion proteins. *Biotechnol Appl Biochem* 2010;56(4):131–40. <https://doi.org/10.1042/BA20100143>. PMID: 20590527.
- [32] Mourelle-Insua Á, Aalbers FS, Lavandera I, et al. What to sacrifice? Fusions of cofactor regenerating enzymes with Baeyer-Villiger monooxygenases and alcohol dehydrogenases for self-sufficient redox biocatalysis. *Tetrahedron* 2019;75(13):1832–9. <https://doi.org/10.1016/j.tet.2019.02.015>.
- [33] Yang H, Liu L, Xu F. The promises and challenges of fusion constructs in protein biochemistry and enzymology. *Appl Microbiol Biotechnol* 2016;100(19):8273–81. <https://doi.org/10.1007/s00253-016-7795-y>. PMID: 27541749.
- [34] Ki MR, Pack SP. Fusion tags to enhance heterologous protein expression. *Appl Microbiol Biotechnol* 2020;104(6):2411–25. <https://doi.org/10.1007/s00253-020-10402-8>. PMID: 31993706.
- [35] Beckmann BM, Castello A, Medenbach J. The expanding universe of ribonucleoproteins: of novel RNA-binding proteins and unconventional interactions. *Pflügers Arch* 2016;468(6):1029–40. <https://doi.org/10.1007/s00424-016-1819-4>. PMID: 27165283.
- [36] Ohno H, Akamine S, Saito H. RNA nanostructures and scaffolds for biotechnology applications. *Curr Opin Biotechnol* 2019;58:53–61. <https://doi.org/10.1016/j.copbio.2018.11.006>. PMID: 30502620.
- [37] Liu Z, Cao S, Liu M, et al. Self-assembled multienzyme nanostructures on synthetic protein scaffolds. *ACS Nano* 2019;13(10):11343–52. <https://doi.org/10.1021/acsnano.9b04554>. PMID: 31498583.
- [38] Fu J, Yang YR, Dhakal S, et al. Assembly of multienzyme complexes on DNA nanostructures. *Nat Protoc* 2016;11(11):2243–73. <https://doi.org/10.1038/nprot.2016.139>. PMID: 27763626.
- [39] Egorov AM, Avilova TV, Dikov MM, et al. NAD-dependent formate dehydrogenase from methylotrophic bacterium, strain 1. Purification and characterization. *Eur J Biochem* 1979;99(3):569–76. <https://doi.org/10.1111/j.1432-1033.1979.tb13289.x>. PMID: 227687.
- [40] Kaup B, Bringer-Meyer S, Sahl H. Metabolic engineering of *Escherichia coli*: construction of an efficient biocatalyst for D-mannitol formation in a whole-cell biotransformation. *Appl Microbiol Biotechnol* 2004;64(3):333–9. <https://doi.org/10.1007/s00253-003-1470-9>. PMID: 14586579.
- [41] Wu SH, Luo XD, Ma YB, et al. Two novel secoergosterols from the fungus *Tylopus plumbeoviolaceus*. *J Nat Prod* 2000;63(4):534–6. <https://doi.org/10.1021/mp990494h>. PMID: 10785434.
- [42] Zeng Y, Dou D, Zhang Y, et al. Rare sugars and antioxidants in *Itea virginica*, *Itea oblonga* Hand.-Mazz., and *Itea yunnanensis* franch leaves. *International Journal of Food Properties* 2015;18(11):2549–2560. [10.1080/10942912.2014.917099](https://doi.org/10.1080/10942912.2014.917099)
- [43] Makower B, Dye WB. Sugar crystallization, equilibrium moisture content and crystallization of amorphous sucrose and glucose. *J Agric Food Chem* 1956;4(1):72–7. <https://doi.org/10.1021/jf60059a010>.
- [44] Lin J, Lee S, Koo Y. Hydrolysis of paper mill sludge using an improved enzyme system. *J Microbiol Biotechnol* 2001;11(3):362–8.
- [45] Li C, Lin J, Gao L, et al. Modeling and simulation of enzymatic gluconic acid production using immobilized enzyme and CSTR–PFTR circulation reaction system. *Biotechnol Lett* 2018;40(4):649–57. <https://doi.org/10.1007/s10529-018-2509-4>. PMID: 29349627.
- [46] Takeshita K, Ishida Y, Takata G, et al. Direct production of allitol from D-fructose by a coupling reaction using D-tagatose-3-epimerase, ribitol dehydrogenase and formate dehydrogenase. *J Biosci Bioeng* 2000;90:545–8. [https://doi.org/10.1016/S1389-1723\(01\)80038-4](https://doi.org/10.1016/S1389-1723(01)80038-4). PMID: 16232907.